# UV-LED irradiation reduces the infectivity of herpes simplex virus type 1 by targeting different viral components depending on the peak wavelength

Thi Kim Ngan Bui [a],[1], Kazuaki Mawatari [a],[*],[1], Takahiro Emoto [b], Shiho Fukushima [a], Takaaki Shimohata [a],[c], Takashi Uebanso [a], Masatake Akutagawa [b], Yohsuke Kinouchi [b], Akira Takahashi [a]

[a] Department of Preventive Environment and Nutrition, Institute of Biomedical Sciences, Tokushima University Graduate School, Kuramoto-cho 3-18-15, Tokushima City, Tokushima 770-8503, Japan
[b] Graduate School of Science and Technology, Tokushima University, Minamijyousanjima-cho 2-1, Tokushima City, Tokushima 770-8506, Japan
[c] Department of Marine Science and Technology, Fukui Prefectural University, 1-1 Gakuen-cho, Obama, Fukui 917-0003, Japan

## ARTICLE INFO

## ABSTRACT

Herpes simplex virus type 1 (HSV-1) is an enveloped virus that mainly infects humans. Given its high global prevalence, disinfection is critical for reducing the risk of infection. Ultraviolet-light-emitting diodes (UV-LEDs) are eco-friendly irradiating modules with different peak wavelengths, but the molecules degraded by UV-LED irradiation have not been clarified. To identify the target viral molecules of UV-LEDs, we exposed HSV-1 suspensions to UV-LED irradiation at wavelengths of 260-, 280-, 310-, and 365-nm and measured viral DNA, protein, and lipid damage and infectivity in host cells. All UV-LEDs substantially reduced by inhibiting host cell transcription, but 260- and 280-nm UV-LEDs had significantly stronger virucidal efficiency than 310- and 365-nm UV-LEDs. Meanwhile, 260- and 280-nm UV-LEDs induced the formation of viral DNA photoproducts and the degradation of viral proteins and some phosphoglycerolipid species. Unlike 260- and 280-nm UV-LEDs, 310- and 365-nm UV-LEDs decreased the viral protein levels, but they did not drastically change the levels of viral DNA photoproducts and lipophilic metabolites. These results suggest that UV-LEDs reduce the infectivity of HSV-1 by targeting different viral molecules based on the peak wavelength. These findings could facilitate the optimization of UV-LED irradiation for viral inactivation.

## 1. Introduction

During pandemics/epidemics, viruses play critical roles in disease development because of their ease of transmission and the associated high number of casualties. Influenza A virus H1N1 subtype caused a pandemic in 1918 that killed at least 50 million people and infected 500 million people globally. Almost all subsequent influenza A strains are derived from the 1918 virus [1]. Human immunodeficiency virus (HIV) has caused an estimated 36.3 million deaths and 79.3 million infections since 1981 [2]. The virus represents an unresolved problem because 37.7 million people were infected by HIV in 2020 [2]. Meanwhile,

severe acute respiratory syndrome coronavirus 2 (SARS-CoV-2) was first detected in 2019, and the number of cases of coronavirus disease 2019 (COVID-19) has increased to 200 million, affecting people in more than 228 countries. More than 4 million people have died of COVID19, and some variants of SARS-CoV-2 have caused global health and public safety crises [3]. Therefore, more efficient disinfection methods are required to limit the spread of viral infectious diseases.

Viruses are small organisms with diameters of 5–300 nm. They have a core of genetic material, either RNA or DNA, surrounded by a protein coat. Some viruses have an envelope cover consisting of phospholipid bilayers. They propagate in host cells after infection. After attachment,

viruses inject their genetic material into host cells, hijack their internal machinery to duplicate themselves, and disrupt cells to release newly formed viral particles. However, some viruses can remain latent after infection before reactivation. Viruses can be transmitted between humans through insects, droplets, and aerosols [4]. Soil, groundwater, wastewater, personal protective equipment, and clothing can also be sources of viral transmission [5,6]. Therefore, the disinfection of environmental viruses is critical for reducing the risk of viral spread. Several disinfection methods with different inactivation mechanisms for viral molecules have been reported. Heat or dry-heat treatments are well established as virucidal methods based on their ability to damage the integrity of capsid and/or envelope proteins [7,8]. These methods are widely applied in the industrial production of materials such as human albumin and milk because of their strong ability to neutralize contaminating bacteria and both enveloped virus and non-enveloped viruses. However, the treatments are not suitable for raw foods and non-thermotolerant materials, and each process must be optimized to protect important protein [7,8]. Low pH-based methods are widely applied for sterilization in biotherapeutic processes [9]. Treatment by acidic solvents or detergents can induce viral inactivation *via* viral envelope destruction, but these treatments cannot inactivate non-enveloped viruses [8,10].

Ultraviolet (UV) irradiation is a common inactivation modality that can damage viral nucleic acids and proteins [7], and it has long been used to disinfect water, air, surfaces, and waste. A low-pressure UV (LP-UV) mercury lamp provides radiation at a monochromatic peak wavelength (254 nm), and it is used for common water treatment processes to remove and inactivate viral and microbial pathogens, mainly by damaging their genomes [11,12]. In recent years, UV light-emitting diodes (UV-LEDs) have been developed as alternative UV light emission sources that can irradiate light of a single wavelength without a filter and that are capable of emitting light at multiple individual wavelengths [13]. UV rays can be classified by wavelength into UVA (315–400 nm), UVB (280–315 nm), and UVC (<280 nm). Currently, the number of reports about the virucidal effects of UVC-LEDs is increasing, revealing that the treatment damaged viral DNA or RNA [14–16]. We recently reported that irradiation by 260-nm UV-LEDs at a fluence of 4.8 mJ/cm$^2$ had stronger virucidal effects on influenza A viruses than that a LP-UV mercury lamp at the same fluence, and the virucidal effect was highly correlated with viral RNA damage but not with hemagglutinin activity [15]. However, some researchers recently suggested that irradiation by UVC-LEDs damaged both viral DNA/RNA and proteins. Tanaka et al. reported that irradiation by 255-nm UV-LEDs at a fluence of 20 mJ/cm$^2$ reduced infectivity by −3 log$_{10}$, the viral RNA load by 43%, and capsid protein levels by 6.9% in a non-enveloped feline calicivirus, and 281-nm UV-LEDs had similar effects on infectivity and the viral RNA load but a stronger effect on capsid protein levels (16.2% reduction) than 255-nm UV-LEDs [17]. Beck et al. reported that a high radiation dose of 400 mJ/cm$^2$ delivered by 261- and 278-nm UV-LEDs reduced protein levels by 11%–34% and 17%–20%, respectively, in a non-enveloped human adenovirus 2 strain [18]. These findings indicate that high-dose irradiation by UVC-LEDs can damage both viral DNA/RNA and proteins in non-enveloped viruses; however, the effects of this treatment on the proteins of enveloped viruses are unclear. In addition, there is little evidence of the virucidal effects of UVB- and UVA-LEDs. We previously demonstrated that irradiation by 310- (0.26 J/cm$^2$) and 365-nm UV-LEDs (6.4 J/cm$^2$) reduced the infectivity of influenza A virus by 90% by inhibiting the replication and transcription of viral RNA in host cells [14]. Minamikawa et al. reported that irradiation (23 mJ/cm$^2$) by 300-nm UV-LEDs reduced the infectivity of SARS-CoV-2 by −4 log [19]. Oguma et al. reported that irradiation (600 mJ/cm$^2$) by 300-nm UV-LEDs reduced the infectivity of feline calicivirus by −4 log [20]. However, the detailed mechanisms of the virucidal effects of UVB- and UVA-LED irradiation have not been elucidated.

Herpes simplex virus type 1 (HSV-1) is an enveloped virus belonging to the Alphaherpesvirinae family that mainly infects humans. HSV-1 has a double-stranded DNA genome that is approximately 152 kilobase pairs in length and covered by an icosahedral capsid. An estimated 3.7 billion people younger than 50 years are infected by HSV-1 globally, and 88% of the population in Africa is infected [21]. Because HSV-1 infects the ocular area as well as other brain regions and other internal organs, many infected patients develop encephalitis or blindness [22,23]. Because HSV-1 highly accumulates in saliva, HSV-1 can spread through both contact and droplet transmission. To reduce viral transmission, irradiation by UV-LEDs could be a reasonable virucidal method for environmental viruses.

Thus, the present study investigated which molecules of HSV-1 were damaged by irradiation by UVA-, UVB-, and UVC-LEDs. We irradiated HSV-1 using 260-, 280-, 310-, and 365-nm UV-LEDs and demonstrated a relationship between the reduction of infectivity and the damage of viral DNA and proteins. To assess viral DNA damage DNA, we measured two DNA photoproducts, namely cyclobutane pyrimidine dimers (CPDs) and 6–4 photoproducts (6-4PPs), which are generated by UV irradiation and which inhibit DNA transcription and replication in other microorganisms [24,25]. To determine the effects of irradiation on viral protein, we measured two viral proteins, specifically glycoprotein D (gD, a glycoprotein present in the envelope with an important role in viral entry into host cells [26]) and infected cell protein 0 (ICP0), by Western blotting. Given that the viral envelope consists of glycoproteins as well as lipids including phosphoglycerolipids and sphingolipids [27,28], we measured the lipophilic metabolites of HSV-1 following UV-LED irradiation by liquid chromatography-time of flight mass spectrometry (LC-TOF-MS). Identification of the virucidal mechanisms and target viral molecules of UV-LEDs at different wavelengths could facilitate the optimization of UV-LED irradiation for viral inactivation.

## 2. Materials and Methods

### 2.1. Cells and Virus Strain

Vero cells and the HSV-1 strain KOS were kindly gifted by Prof. Akio Adachi (Tokushima University Graduate School and Kansai Medical University). Vero cells were cultured in Dulbecco's modified Eagle's medium (DMEM) containing 10% fetal bovine serum (Thermo Fisher Scientific, Waltham, MA, USA) and 50 μg/mL gentamicin (Fujifilm Wako Chemicals, Osaka, Japan) at 37 °C in an atmosphere of 5% CO$_2$. The viral suspensions were prepared for irradiation experiments by propagating HSV-1 in Vero cells for 48 h. The supernatant of culture medium was precleared by centrifugation at 3300 ×*g* for 5 min followed by filtration through 0.45-μmϕ pore membrane filters. The supernatant was then purified by centrifugation at 112,500 ×*g* for 2 h using a CP50 ultracentrifuge with a P40ST angle rotor (Eppendorf Himac Technologies, Ibaragi, Japan) through PBS containing 20% sucrose, as previously reported [15]. The viral pellets were collected and stored at −80 °C until UV-LED irradiation experiments.

### 2.2. Irradiation of Viral Suspensions by UV-LEDs

UV-LEDs (Nichia, Tokushima, Japan) were used to irradiate the viral suspensions at four different wavelengths, namely 365 (NVSU233A-U365), 310 (NCSU234A-U310), 280 (NCSU234A-U280), and 260 nm (MO2257-U260) (Supplementary Fig. S1A). The individual LEDs were placed on a printed circuit board (Audio-Q, Shizuoka, Japan) and connected in series to a current-controlling single power source (PAS40–9, Kikusui Electronics Corp., Kanagawa, Japan). The UV spectral fluence rates (mW/cm$^2$/nm) on the surface of samples were measured six times during UV-LED irradiation using an MCPD 3700A multiple wavelength photometer (Otsuka Electronics, Osaka, Japan). The fluence rates were calculated as the sum of the averaged spectral fluence rates between 200 and 400 nm. The diodes irradiated the viral suspensions under maximum forward current (IF) according to the manufacturer's instructions, and the fluence rates were 106 (365 nm), 4.4 (310 nm), 2.5
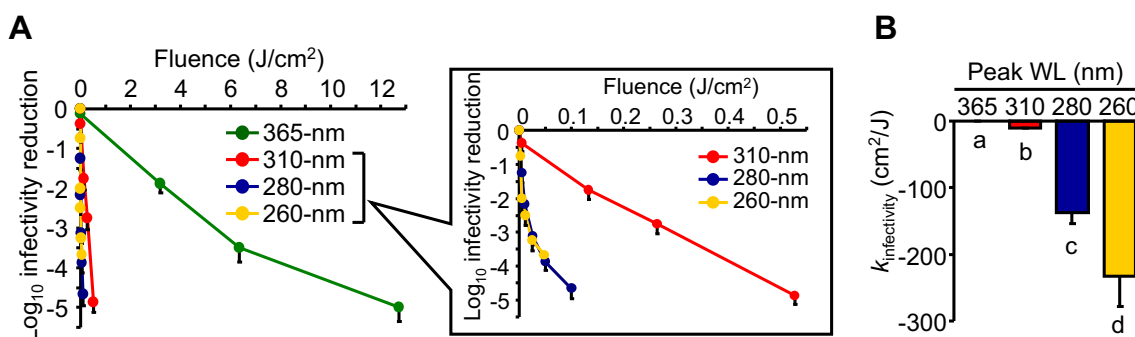
**Fig. 1.** Reduction of the infectivity of herpes simplex virus type 1 (HSV-1) by irradiation with ultraviolet-light-emitting diodes (UV-LEDs) at different peak wavelengths. (A) $\log_{10}$ infectivity reduction following irradiation by UV-LEDs. (B) $K_{titer}$ for each UV-LED type. The viral suspensions of HSV-1 were irradiated by four UV-LEDs with different peak wavelengths, and the viral titers were measured as the median tissue culture infectious dose in Vero cells, as described in the Materials and Methods. $K_{titer}$ was calculated as the ratio of the $\log_{10}$ infectivity reduction to the irradiation fluence of each UV-LED type. Values are presented as the mean ± SD ($n = 4$). Different letters indicate a statistical difference ($P < 0.05$) compared to the other values using ANOVA with Bonferroni's multiple comparison test. WL, wavelength.

(280 nm), and 1.2 mW/cm$^2$ (260 nm). The UV-LEDs emitted radiation downward onto the surface of the viral suspensions (Supplementary Fig. S1B). The viral suspensions were irradiated for 30, 60, or 120 s by both 365- and 310-nm UV-LEDs or for 4, 10, 20 s by both 280- and 260-nm UV-LEDs.

### 2.3. Measurements of Virus Infectivity

A median tissue culture infectious dose (TCID$_{50}$) assay was performed in Vero cells to determine the cytoplasmic effect of HSV-1. After UV-LED irradiation of the viral suspensions ($1.74 \times 10^7$ TCID$_{50}$/mL), Vero cells cultured in DMEM in 48-well plates were infected with 10-fold serial dilutions of the viral suspensions and incubated at 37 °C. An un-irradiated viral suspension was used as a dark control. Following 72 h of incubation, the cells were stained with 0.5% crystal violet solution containing 10% formalin for TCID$_{50}$ analysis. The viral-inactivating effects of UV-LED irradiation were assessed using the $\log_{10}$ infectivity reduction, which was calculated as follows: log TCID$_{50}$/mL ratio = $\log_{10}(N_t/N_0)$, where $N_t$ is TCID$_{50}$/mL of the UV-irradiated sample and $N_0$ is TCID$_{50}$/mL of the sample without UV irradiation. $K_{infectivity}$ was calculated as the ratio of the $\log_{10}$ infectivity reduction to the fluence of each UV-LED type.

### 2.4. RNA Extraction from Vero Cells and Reverse Transcription (RT)-Quantitative Real-Time Polymerase Chain Reaction (qPCR)

The mRNA levels of the HSV-1 *pol* gene in infected cells were measured by RT-qPCR. Vero cells in a six-well plate were infected with viral suspensions following UV-LED irradiation or no treatment (dark control). At 2, 4, and 6 h post-infection (hpi), the cells were washed three times with ice-cold PBS, and total RNA was extracted and purified using TRIzol® Reagent (Thermo Fisher Scientific) according to the manufacturer's instructions. The total RNA concentration was quantified spectrophotometrically (Beckman Coulter, Brea, CA, USA). The RT reaction was performed with 500 ng of purified RNA and both random hexamer and oligo(dT) primers using a First Strand cDNA synthesis kit (TaKaRa Bio, Shiga, Japan). Real-time PCR was performed using a LightCycler® 2.0 Real-Time PCR System (Roche, Mannheim, Germany) as previously described [24,25]. The primers for HSV-1 *pol* (forward, 5′-GCTCGAGTGCGAAAAAACGTTC-3′; reverse, 5′-CGGGGCGCTCGGCTAAC-3′) were used to quantify the total viral RNA level in Vero cells. *Act-b* (forward, 5′-AAGGATTCA-TATGTGGGCGATG-3′; reverse, 5′-TCTCCATGTCGTCCCAGTTGGT-3′) was used as an internal control for host cellular RNA.

### 2.5. Dot-Blot Analysis

Viral DNA was purified from the viral suspensions with or without UV-LED irradiation using a Viral Nucleic Acid Extraction Kit (Favorgen, Ping-Tung, Taiwan) according to the manufacturer's instructions. The concentrations of viral DNA were quantified spectrophotometrically and checked by agarose gel electrophoresis. The purified viral DNA was filtered through a 0.45-μmϕ pore nitrocellulose membrane (Fujifilm Wako Chemicals) using the Bio-Dot SF Microfiltration Apparatus (Bio-Rad Laboratories, Hercules, CA, USA). The membrane was dried at 37 °C and then incubated with 5% bovine serum album in Tris-buffered saline containing Tween 20 (TBS-T) for 1 h to block non-specific immuno-reaction. The membrane was incubated with anti-CPD or anti-6-4PP antibody (Cosmo Bio, Tokyo, Japan) at 4 °C for 12 h. The membranes were washed three times with TBS-T and incubated with horseradish peroxidase-conjugated anti-mouse immunoglobulin antibody (MBL, Nagoya, Japan) for 1 h. The immunoreactions were visualized using an enhanced chemiluminescence detection system (Amersham Biosciences, Buckinghamshire, UK). The images were captured by the LAS-3000UV mini CCD camera system, (Fujifilm, Tokyo, Japan) and analyzed densitometrically using Scion Image software (Scion Corporation, Frederick, MD, USA). $K_{CPDs}$ and $K_{6-4PPs}$ were calculated as the ratios of the levels of each photoproduct to the $\log_{10}$ reduction of infectivity induced by each UV-LED type.

### 2.6. Western Blotting

Following UV-LED irradiation or no treatment, the viral suspensions were homogenized with lysis buffer, and the protein levels were determined by Western blotting as previously described [29]. Anti-gD and anti-ICP0 antibodies were purchased from Santa Cruz Biotechnology (Santa Cruz, CA, USA). $K_{ICP0}$ and $K_{gD}$ were calculated as the ratios of the immunoblot values of each protein to the reduction of the viral titer induced by each UV-LED type.

### 2.7. Measurement of Lipophilic Metabolites in HSV-1

The lipophilic fractions of the viral suspensions were isolated using the Bligh and Dyer method [30]. The fractions were analyzed using an Agilent LC-TOFMS 6200 with a ZORBAX Eclipse Plus C18 column (Agilent Technologies, Palo Alto, CA, USA) at a flow rate of 1 mL/min using water:methanol (40:60) as the initial mobile phase. After sample injection, the percentage of methanol was increased to a water:methanol ratio of 0:100 at 10–30 min and was continued for 20 min. The equipped ion source of MS was the Agilent Jetstream electrospray ionization source (Dual AJS ESI, Agilent Technologies). The electrospray ionization
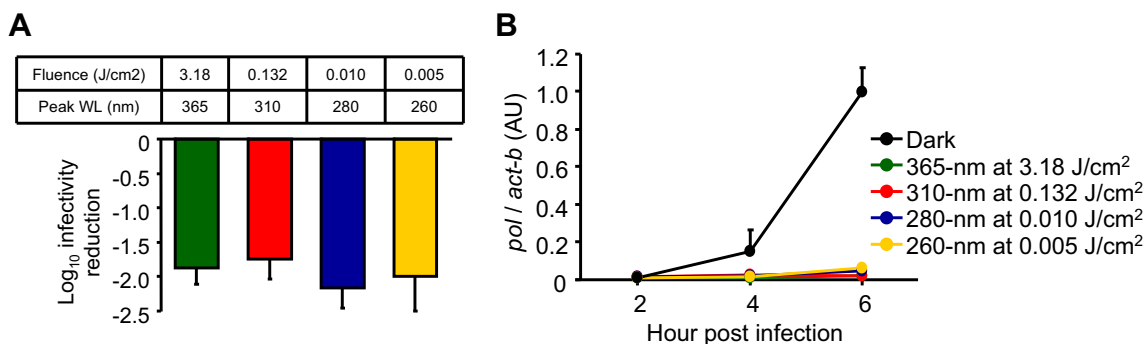
**Fig. 2.** Effect of irradiation by each ultraviolet-light-emitting diode (UV-LED) type on the transcription of HSV-1 genes in host cells. (A) $\log_{10}$ infectivity reduction following irradiation by each UV-LED type at the indicated fluences. (B) The mRNA levels of HSV-1 *pol* in Vero cells. The viral suspensions were irradiated by each UV-LED type, which reduced infectivity by approximately $-2 \log_{10}$, and then used to infect Vero cells. The mRNA levels of *pol* in Vero cells at the indicated time after infection were measured by reverse transcription-quantitative real-time polymerase chain reaction, as described in the Materials and Methods. Values are presented as the mean $\pm$ SD ($n = 3$). AU, arbitrary unit; WL, wavelength.
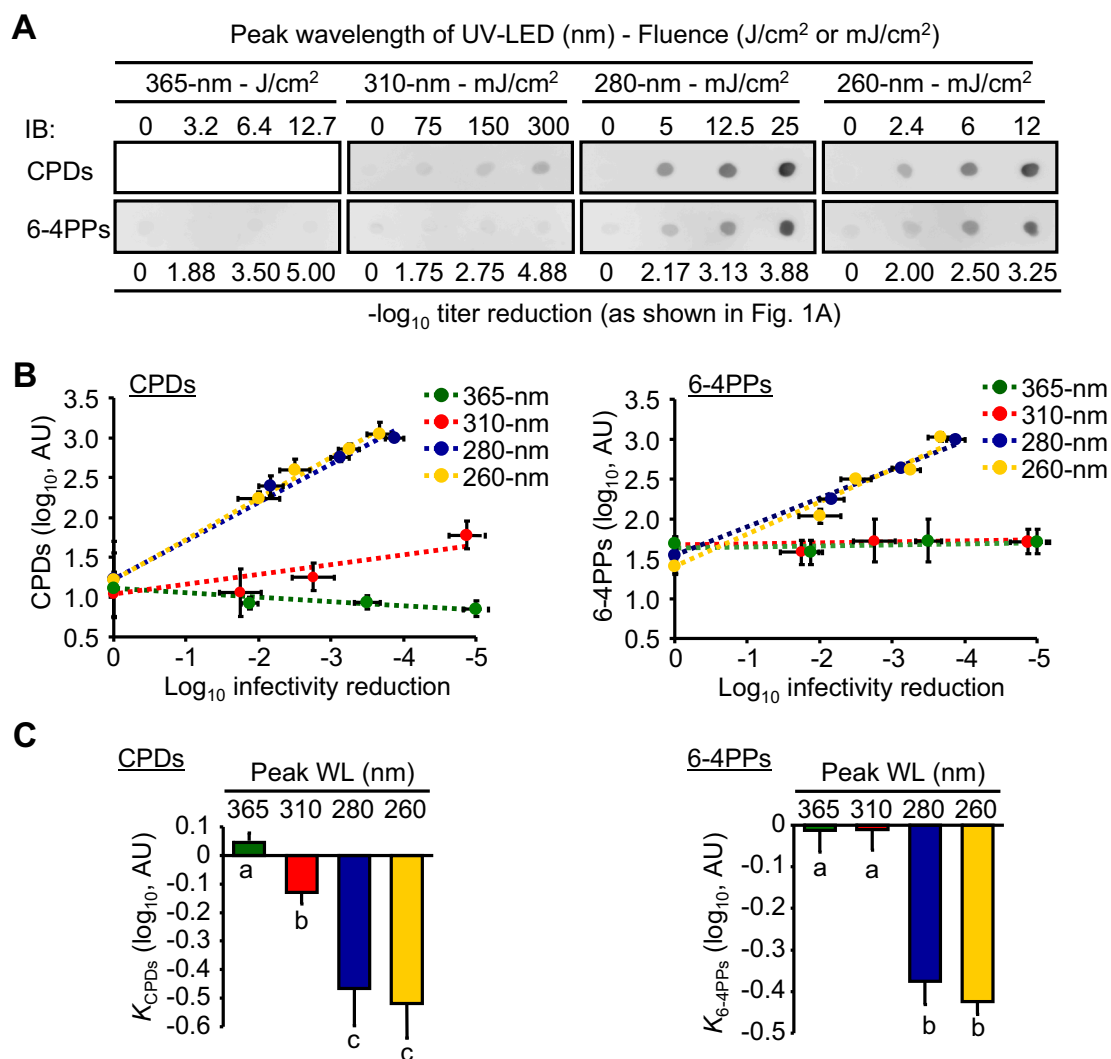


**Fig. 3.** The levels of viral DNA photoproducts induced by exposure to ultraviolet-light-emitting diode (UV-LED) irradiation. (A) Representative images of immunoblotting for cyclobutane pyrimidine dimers (CPDs) and 6–4 photoproducts (6-4PPs). (B) The correlations between the levels of DNA photoproducts and $\log_{10}$ infectivity reduction induced by each UV-LED type. (C) $K_{CPDs}$ and $K_{6-4PPs}$ of each UV-LED type. Viral DNA was extracted from viral suspensions following irradiation by four UV-LED types at the indicated fluences. The DNA photoproducts were detected by dot-blot analysis using anti-CPD and anti-6-4PP antibodies, as described in the Materials and Methods. $K_{CPDs}$ and $K_{6-4PPs}$ were calculated as the ratios of the levels of the DNA photoproducts to the $\log_{10}$ infectivity reduction. Values are presented as the mean $\pm$ SD ($n = 4$–6). Different letters indicate a statistical difference ($P < 0.05$) compared to the other values using ANOVA with Bonferroni's multiple comparison test.

source was operated in the positive mode with spray voltages of 3500 V for the capillary entrance and 500 V for the nozzle, a nitrogen sheath gas temperature of 250 °C at a flow rate of 12 L/min, a nitrogen drying gas temperature of 150 °C at a flow rate of 10 L/min, and a nitrogen nebulizer at 45 psig. Purified ubiquinone-8 from *Escherichia coli* (Avanti Polar Lipids, Alabaster, AL, USA) was used as the internal standard to calculate the recovery rate during sample purification. The *m/z* values, retention times, and ion counts of metabolites were extracted from the total ion chromatogram using the Molecular Future Extraction method of MassHunter software (Agilent Technologies). The metabolites that significantly differed between the dark control and UV-LED–irradiated samples ($P < 0.05$ by one-way analysis of variance [ANOVA]) were selected by multivariate analysis using Mass Profiler Professional software (Agilent Technologies). The selected metabolites were identified using the METLIN Personal Metabolite Database (Agilent Technologies). The metabolites were categorized by LIPID MAPS® (Wellcome Trust, London, UK).

### 2.8. Statistical Analysis

The statistical analysis of differences was performed by ANOVA with Bonferroni's multiple comparison test using Statview 5.0 software (SAS Institute Inc., Cary, NC, USA). Student's *t*-test was used for paired data where appropriate. $P < 0.05$ indicated statistical significance according to the analysis performed. Spearman's rank correlation test was used to analyze the association between the infectivity reduction and the levels of viral DNA photoproducts or viral proteins in each UV-LED group.

## 3. Results and Discussion

### 3.1. Irradiation by each UV-LED Reduced the Infectivity of HSV-1

To compare the virucidal effects of UV-LEDs with different peak wavelengths, we irradiated viral suspensions using 260-, 280-, 310- and 365-nm UV-LEDs and measured the infectivity of the virus in host cells (Fig. 1). All UV-LEDs reduced the infectivity of HSV-1 in a fluence-dependent manner by as much as approximately $-4$ $\log_{10}$ (Fig. 1A). $K_{\text{infectivity}}$ indicated that 260-nm UV-LEDs had the highest virucidal efficiency among the UV-LEDs used in this study (Fig. 1B). Meanwhile, 310- and 365-nm UV-LEDs had significantly lower efficiency than UVC-LEDs. These results illustrated that the peak wavelength was an important factor of the virucidal efficiency induced by UV-LED irradiation.
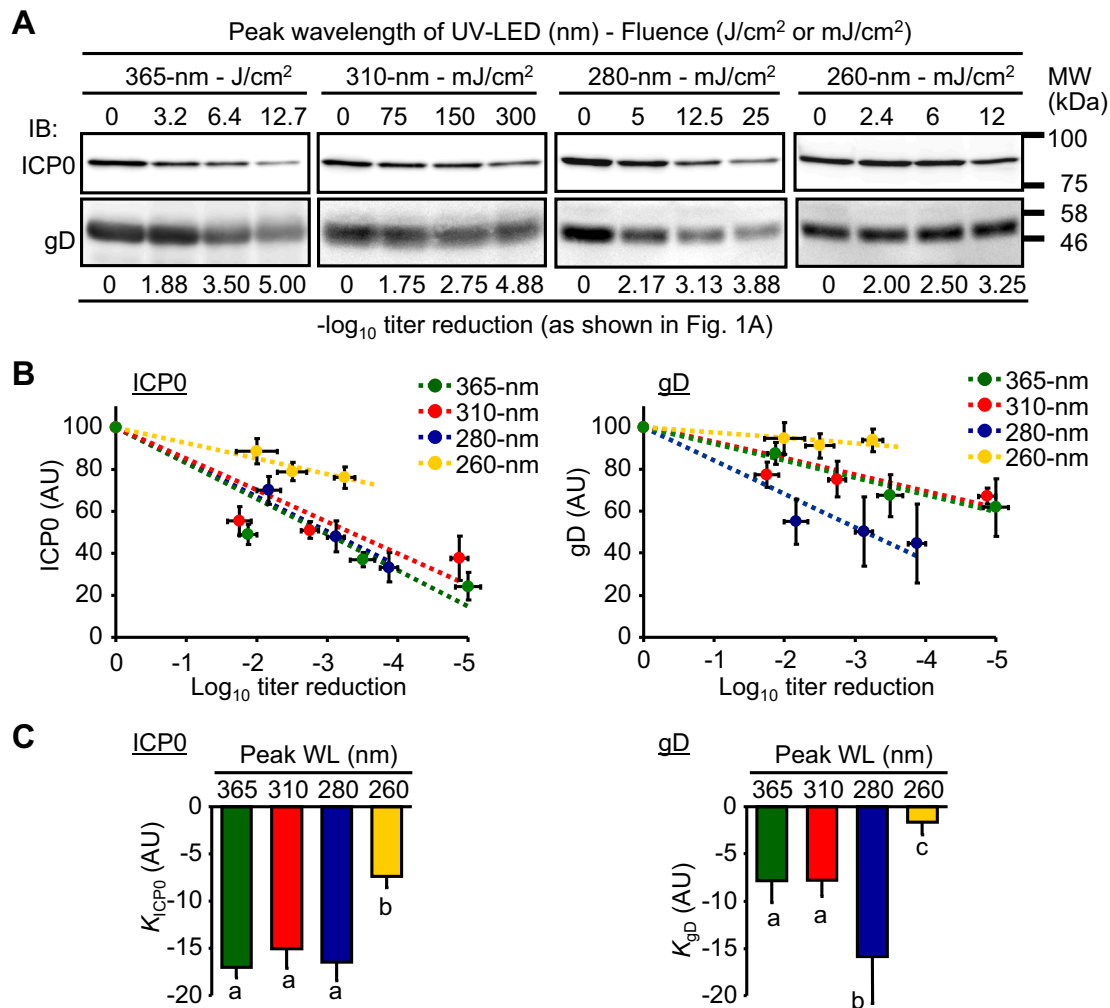


**Fig. 4.** The effect of ultraviolet-light-emitting diode (UV-LED) irradiation on viral protein levels in HSV-1. (A) Representative images of immunoblotting for ICP0 and gD. (B) The correlations between the levels of ICP0 or gD and the $\log_{10}$ viral titer reduction. (C) $K_{\text{ICP0}}$ and $K_{\text{gD}}$ for each UV-LED type. Proteins were extracted from HSV-1 suspension irradiated using four UV-LED types at the indicated fluences. The viral proteins were detected by Western blotting using anti-ICP0 and anti-gD antibodies, as described in the Materials and Methods. $K_{\text{ICP0}}$ and $K_{\text{gD}}$ were calculated as the ratio of the protein levels to the $\log_{10}$ viral titer reduction. Values are presented as the mean ± SE ($n = 3$–4). Different letters indicate a statistical difference ($P < 0.05$) compared to the other values using ANOVA with Bonferroni's multiple comparison test.

## 3.2. Irradiation by each UV-LED Type Inhibited the HSV-1 Gene Transcription in Host Cells

Next, to check whether irradiation by UV-LEDs inhibited the transcription of HSV-1 in host cells, we measured the mRNA levels of *pol* at 2, 4, and 6 hpi. The viral suspensions were irradiated by each UV-LED type at 3.16 (365 nm), 0.132 (310 nm), 0.01 (280 nm), and 0.005 J/cm$^2$ (260 nm), all of which reduced infectivity by approximately $-2$ $\log_{10}$ (Fig. 2A), and the suspensions were then used to infect Vero cells. The mRNA levels of *pol* in host cells infected with unirradiated viral suspensions were increased at 4 and 6 hpi (Fig. 2B). Irradiation by each UV-LED type significantly inhibited the upregulation of *pol* in host cells (Fig. 2B). In addition, the levels of *pol* in host cells were not significantly different at each time point among the four UV-LEDs. We previously reported that irradiation by 280-, 310-, and 365-nm UV-LEDs inhibited the transcription and replication of the viral RNA of influenza A virus in host cells [14]. The current results suggest that irradiation by each UV-LED type inhibits the transcription of enveloped virus genes in host cells.

## 3.3. The Levels of Viral DNA Photoproducts Following Irradiation by UVC-LEDs Were Highly Correlated with the Reduction of Infectivity

To assess HSV-1 genomic DNA damage induced by UV-LED irradiation, we evaluated the levels of the DNA photoproducts CPDs and 6-4PPs. Formation of the photoproducts leads to changes of the conformations of the DNA helix [31] and inhibition of DNA transcription and replication in bacteria such as *E. coli and Staphylococcus aureus* [24,25]. However, few reports have examined the effects of these DNA photoproducts on the viral genome. The levels of both CPDs and 6-4PPs were increased by irradiation by 260- and 280-nm UV-LEDs in a fluence-dependent manner ($R > 0.98$, $P < 0.01$, Fig. 3A–B), suggesting that the virucidal effects of 260- and 280-nm UV-LEDs might depend on viral genomic DNA damage. In addition, the ratios of the level of each photoproduct to the $\log_{10}$ infectivity reduction ($K_{CPDs}$ and $K_{6-4PPs}$) were not significantly different between irradiation with 260- and 280-nm UV-LEDs (Fig. 3C). Our data were supported by the results of Matsunaga et al., who reported that irradiation by monochromatic UV at 260 and 280 nm generated similar levels of DNA photoproducts [32]. Furthermore Yamada et al. determined that 270 nm was highest peak wavelength in the absorption spectrum of thymine [33]. From these results, 270-nm UV may have the strongest effect on the formation of DNA photoproducts in HSV-1.

Irradiation by 310-nm UV-LEDs statistically increased CPD levels in a fluence-dependent manner ($R = 0.93$, $P < 0.01$), but $K_{CPDs}$ of 310-nm UV-LEDs was significantly lower than those of 260- and 280-nm UV-LEDs. Nascimento et al. reported that UVB irradiation induced CPD formation in the conidia of fungi including *Aspergillus fumigatus* and *Metarhizium acridum* in a fluence-dependent manner [34]. Bastien et al. also demonstrated that CPDs were the main photoproducts in both purified DNA and human fibroblasts following UVB irradiation at 40 J/cm$^2$ [35]. Furthermore, Douki et al. demonstrated that irradiation by monochromatic UV at 320 nm increased 6-4PP levels, but its levels were 500-times lower than those of CPDs [36,37]. However, the fluences of UVB irradiation in these reports were significantly higher than that of 310-nm UV-LEDs in this study. Unlike the results for CPD levels, irradiation by 310-nm UV-LEDs did not change 6-4PP levels (Fig. 3B–C). These findings suggest that CPDs are the primary photoproducts generated following UVB irradiation in viruses and other microorganisms, but the generation of CPDs in response to 310-nm UV-LED irradiation may have a smaller contribution to the reduction of HSV-1 infectivity than that induced by 260- and 280-nm UV-LEDs.

Irradiation by 365-nm UV-LEDs had no effect on the levels of both photoproducts. However, some reports demonstrated that UVA irradiation increased the levels of the photoproducts in other microorganisms. Tyrrell demonstrated that radiation at a wavelength of 365 nm (1350 J/cm$^2$) increased the levels of pyrimidine dimers in the DNA of *E. coli* [38].

Mouret et al. also reported that UVA irradiation at 100 J/cm$^2$ increased CPD levels but not 6-4PP levels in *Micrococcus luteus* and *Clostridium perfringens* [39]. In this study, HSV-1 was irradiated by 365-nm UV-LEDs at fluences up to 12.7 J/cm$^2$. The results suggested that the fluence of 365-nm UV-LED radiation in this study were not sufficient to increase CPD levels in HSV-1. In addition, the levels of CPDs induced by monochromatic UV irradiation at 350 nm were approximately 100,000-fold lower than those induced by UV irradiation at 260 nm [36]. From these results, viral DNA damage induced by 365-nm UV-LED irradiation might have had a small contribution to the observed reduction of HSV-1 infectivity.

## 3.4. Degradation of Viral Proteins by UV-LED Irradiation Was Correlated with the Infectivity Reduction

To assess HSV-1 protein damage induced by UV-LED irradiation, we evaluated the levels of ICP0 and gD by Western blotting (Fig. 4). Irradiation by 280-, 310-, and 365-nm UV-LEDs significantly decreased the levels of both ICP0 and gD in a fluence-dependent manner (Fig. 4A), and the levels of both HSV-1 proteins were highly correlated with the $\log_{10}$ infectivity reduction (Fig. 4B). These results suggested that the virucidal effects of 280-, 310-, and 365-nm UV-LEDs were dependent on viral protein damage. These results were supported by the findings of Beck et al., who reported that UV irradiation at various peak wavelengths within the range of 200–300 nm decreased protein levels in human adenovirus serotype 2 [18]. However, few reports have evaluated the effects of UVB and UVA irradiation on viral protein levels. However, some previous reports demonstrated that UVB and UVA irradiation changed protein modifications in gram-negative bacteria. Bosshard et al. demonstrated that UVA irradiation induced protein oxidation and aggregation in *E. coli* [40]. Santos et al. reported that UVB irradiation induced oxidative modification of the side chains of aromatic amino acids, including tyrosine and tryptophan, in the proteins of *Pseudomonas sp.* [41] The enveloped glycoprotein gD has an important role in viral entry into host cells *via* binding to cognate receptors such as nectin-1 and nectin-2 [42]. ICP0 acts as a viral interferon antagonist and participates in the reversal of HSV-1 silencing [43]. The degradation of gD and ICP0 may be important for the reduction of infectivity induced by UV-LED irradiation.

$K_{ICP0}$ did not significantly differ among irradiation with 280-, 310-, and 365-nm UV-LEDs, but $K_{gD}$ of 280-nm UV-LEDs was higher than those of 310- and 365-nm UV-LEDs (Fig. 4C). In addition, irradiation by 260-nm UV-LEDs moderately decreased ICP0 levels in a fluence-dependent manner ($R > 0.75$, $P < 0.01$), but it had no effect on gD levels. From these results, ICP0 and gD had different sensitivities to UV-LED irradiation. The amino acid (AA) sequences of proteins represent an important factor for photon absorption and conformational changes of proteins [44]. Charged AAs including lysine, glutamate, and arginine had broad absorption features extending beyond 320 nm [45]. Conversely, aromatic AAs have distinct absorption features because of the presence of chromophores in the side chains, and the wavelengths of peak absorption for tryptophan, tyrosine, and phenylalanine are 280, 275, and 257 nm, respectively [45]. The ratios of charged AAs to total AAs do not differ between gD and ICP0, but the content of aromatic AAs in gD (33/394) is higher than that in ICP0 (23/776). These results suggest that the content of aromatic AAs may be an important factor for protein degradation induced by 280-nm UV-LED irradiation. In addition to aromatic AAs, disulfide bonds in proteins represent another important factor the sensitivity to UV irradiation [46]. According to DiANNA 1.1 disulfide bond prediction software [46], ICP0 has three putative half-cysteines involved in disulfide bonds, whereas gD has none. Wongkongkathep et al. demonstrated that 266-nm UV irradiation enhanced protein cleavage through disulfide bond degradation [47]. These data suggest that the differing sensitivities of ICP0 and gD to 260-nm UV-LED irradiation might be associated with the presence of disulfide bonds.
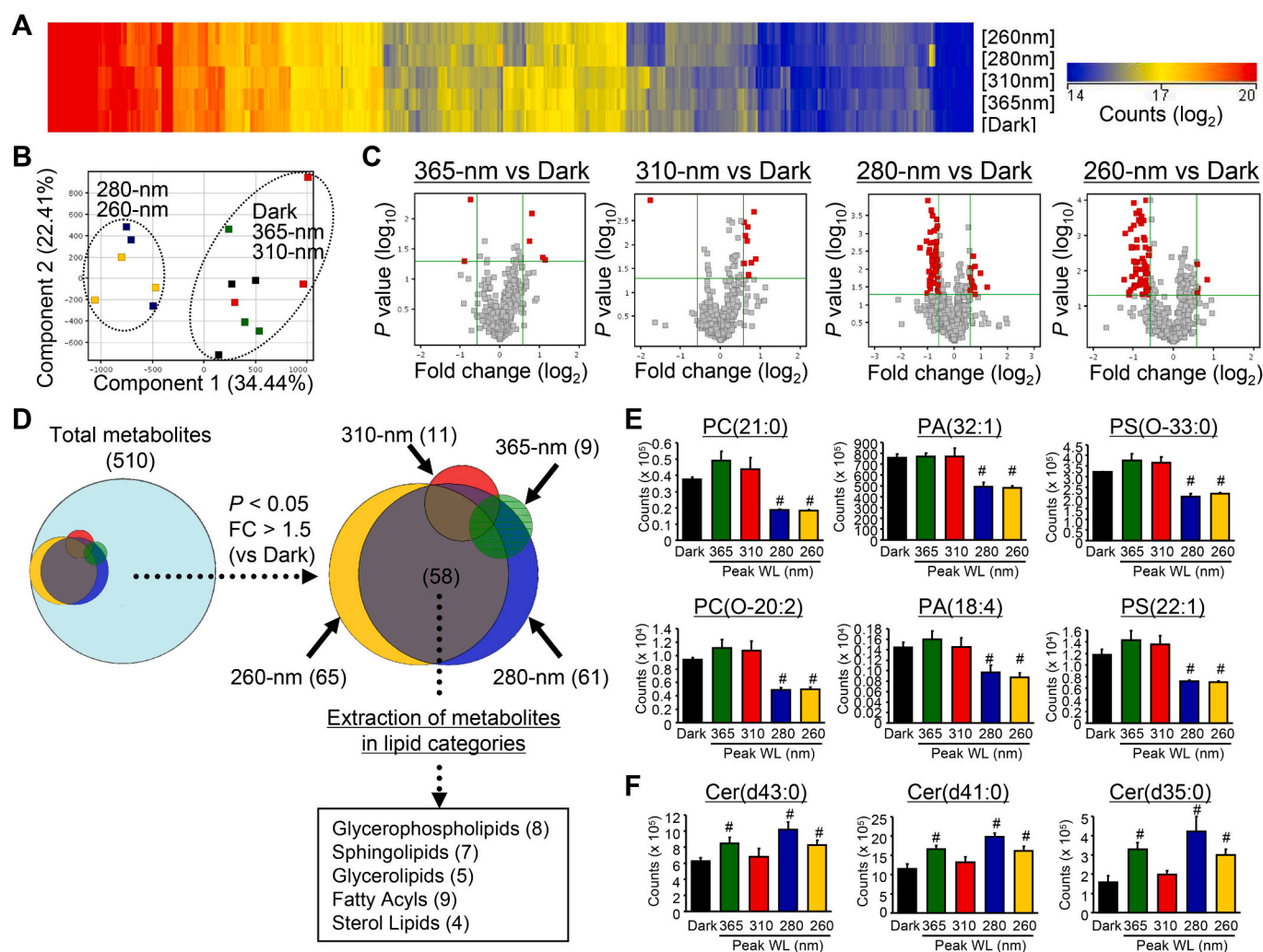
**Fig. 5.** The effect of ultraviolet-light-emitting diode (UV-LED) irradiation on lipid metabolites in herpes simplex virus type 1 (HSV-1). (A) Heat map presenting the values of 510 lipophilic metabolites in each UV-LED group. (B) Principal component analysis of the metabolite datasets from each UV-LED group. (C) Volcano plot analyses of the metabolite values between each UV-LED group and the dark control. Red plots indicate significant differential metabolites between the dark control and irradiation groups using Student's *t*-test ($P < 0.05$, fold change >1.5). (D) Venn diagram presenting the number of differential metabolites between each UV-LED group and the dark control. (E, F). The levels of glycerophospholipid (E) and sphingolipid (F) species in each UV-LED group. The lipophilic metabolites were extracted from the HSV-1 suspensions after UV-LED irradiation and measured by liquid chromatography-time of flight mass spectrometry, as described in the Materials and Methods. Each UV-LED type reduced viral infectivity at the indicated fluence by approximately −3 $\log_{10}$, as presented in Supplementary Fig. S3A. Values are presented as the mean ± SE ($n = 4$–5). #$P < 0.05$ for each UV-LED *vs.* the dark control using one-way ANOVA. PC, phosphatidylcholine; PA, phosphatidic acid; PS, phosphatidylserine; Cer, ceramide. (For interpretation of the references to colour in this figure legend, the reader is referred to the web version of this article.)

### 3.5. Irradiation by UVC-LEDs Modified the Profile of Viral Lipid Metabolites

To evaluate the effect of UV-LEDs on the lipids of HSV-1, we measured lipid metabolites by LC-TOF-MS. We extracted lipophilic fractions from HSV-1 suspensions after irradiation by each UV-LED type at the fluence that induced an approximately −3 $\log_{10}$ infectivity reduction (Supplementary Fig. S3A). Fig. 5A presents the heat map of the values of 510 metabolites detected in all samples. Principal component analysis indicated that the profile of the metabolites was changed by 260- and 280-nm UV-LED irradiation, but not by 310- and 365-nm UV-LED irradiation (Fig. 5B). The volcano plot analysis illustrated that 65 (260-nm UV-LEDs), 61 (280-nm UV-LEDs), 11 (310-nm UV-LEDs), and 9 (365-nm UV-LEDs) metabolites were statistically changed ($P < 0.05$, fold change >1.5) by irradiation (Fig. 5C–D). The differential metabolites induced by irradiation by 260- and 280-nm UV-LEDs were highly merged and included glycerophospholipids, sphingolipids, glycerolipids, fatty acyls, and sterol lipids (Fig. 5D). Previous

reports illustrated that phosphoglycerolipids and sphingolipids were the main lipids in the envelopes of influenza A viruses and HIV [27,28]. In this study, irradiation by both 260- and 280-nm UV-LEDs decreased the levels of some phosphoglycerolipid species including phosphatidylcholines [PC(21:0), PC(O-20:2)], phosphatidic acids [PA(32:1), PA(18:4)], and phosphatidylserines [PS(O-33:0), PS(22:1)] (Fig. 5E). Among sphingolipids, 260-, 280-, and 365-nm UV-LED irradiation increased the levels of ceramide species including Cer(d43:0), Cer(d41:0), Cer(d38:0), and Cer(d35:0) (Figs. 5E and S3B), whereas 260- and 280-nm UV-LED irradiation decreased the levels of two phosphatidylethanol-ceramides, namely PE-Cer(d34:2) and PE-Cer(d35:2) (Fig. S2B). The absorbance of phospholipids peaked at 203 nm with parallel variations in the wavelength range of 190–290 nm [48]. Chatterjee et al. demonstrated that 254- or 256-nm UV irradiation at a similar fluence as used in this study induced lipid peroxidation in the liposomal membrane of phospholipid-containing liposomes and goat erythrocytes [49,50]. In addition, Grether-Beck et al. reported that UVA radiation at 30 J/cm$^2$ and singlet oxygen increased ceramide levels in protein-free,
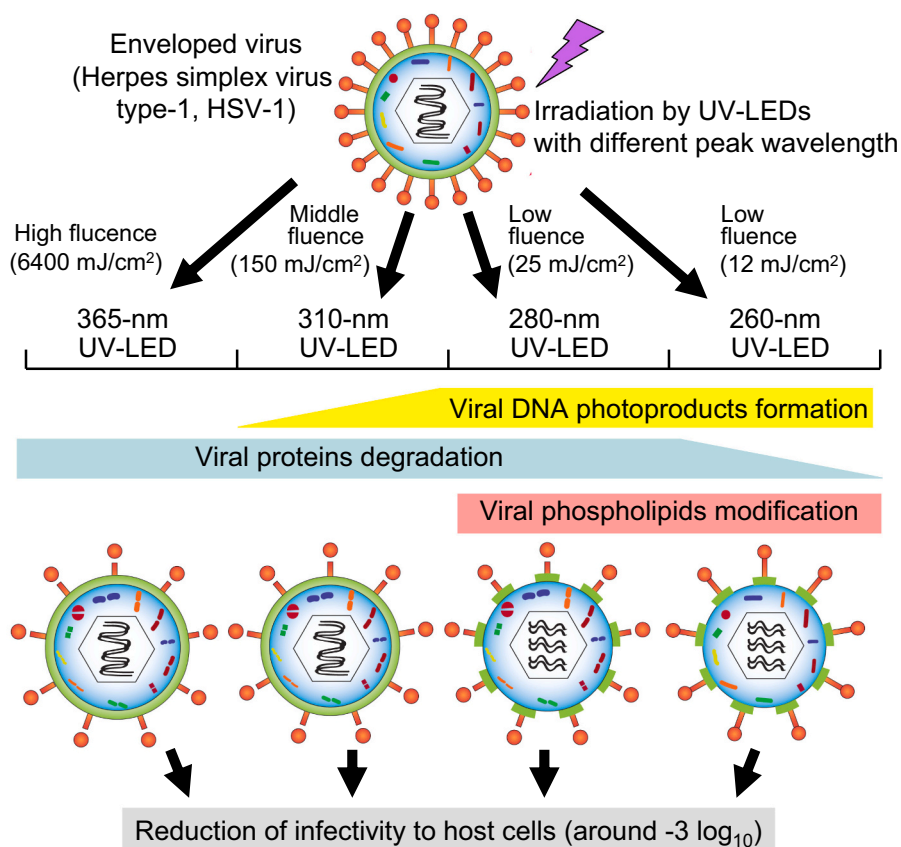
**Fig. 6.** Schematic summary of this study.

sphingomyelin-containing liposomes *via* reactive oxygen intermediates as singlet oxygen [51]. From these reports, the modification of viral glycerophospholipids and ceramides by UV-LED irradiation might depend on lipid peroxidation. However, few reports have discussed the degradation of viral lipids by UV irradiation. Further evidence is needed to clarify the mechanisms by which UV-LED irradiation modifies viral lipids.

The roles of phosphoglycerolipids and sphingolipids in the viral envelope are not well understood. Some phosphoglycerolipid-binding proteins in host cells were identified to have important roles in cell entry and infection by enveloped viruses [52]. Huang et al. reported that antiserum against annexin V, a widespread phosphoglycerolipid-binding protein, completely inhibited the infectivity of influenza A virus [53]. Meertens et al. demonstrated that the phosphatidylserine-binding protein families T-cell immunoglobulin and mucin domain and Tyro3, Axl and MerTK receptor tyrosine kinase mediated the entry of dengue viruses into host cells, but they did not mediate the entry of HSV-1 [54]. No phosphoglycerolipid-binding proteins involved in HSV-1 infection have been identified. Phosphoglycerolipids and sphingolipids on the viral envelope and membranes in host cells have important roles in virus infection. Arii et al. reported that phosphatidylethanol biosynthesis mediated by phosphate cytidylyltransferase 2, ethanolamine was required for efficient HSV-1 envelopment in host cell and viral replication [55]. Audi et al. reported sphingomyelin depletion in both the plasma membrane and virus envelope by treatment with exogenous bacterial sphingomyelinase impaired virus infection and reduced host entry by influenza A virus [56]. From these results, modification of viral phospholipids by UV-LED irradiation might contribute to the inhibition of HSV-1 entry into host cells and viral replication.

To inactivate viral and microbial pathogens, genomic DNA/RNA is well known as a main target of UVC irradiation [13,14]. In this study, we

elucidated that UVC-LEDs induced the formation of DNA photoproducts and modification of viral proteins and phospholipids. Unlike UVC-LEDs, 310- and 365-nm UV-LEDs mainly target viral proteins because they decreased the levels of viral proteins in a fluence-dependent manner, but the levels of DNA photoproducts and profile of lipophilic metabolites were not dualistically changed. In this study, 260-nm UV-LEDs had the most efficient virucidal effect among the UV-LEDs (Fig. 1), but protein degradation induced by 260-nm UV-LED had a minor contribution to the reduction of infectivity (Fig. 4). Because the external quantum efficiencies of aluminum gallium nitride-based deep UVC-LEDs are <10%, a strategy to increase the efficiency of viral inactivation by deep UVC-LEDs is necessary for their application against environmental viruses. Our results indicate that combined treatment by different UV-LEDs might be a reasonable method to increase the virucidal effect through targeting different viral molecules. We previously reported that the combination of 365-nm UV-LED and LP-UV lamp irradiation exerted a synergistic bactericidal effect on *Vibrio parahaemolyticus* that was dependent on the suppression of CPD repair [24]. Our previous data were supported by the findings of Xiao et al. and Song et al., who reported the synergistic inactivating effects of combined 265-nm/365-nm UV-LED irradiation on *E. coli* through the suppression of DNA repair [57,58]. However, some reports illustrated that the combination of 265-nm/280-nm UV-LEDs had no synergistic effect on *E. coli* [58,59]. These findings suggest that the combination of 260- and 365-nm UV-LEDs would be useful for both bacteria and enveloped viruses; however, more evaluations are necessary for the application of combined UV-LEDs for viral inactivation.

## 4. Conclusion

In this study, we irradiated HSV-1 suspensions using UV-LEDs with four different peak wavelengths (260-, 280-, 310-, and 365-nm) and

measured the reduction of infectivity and damage of viral molecules including DNA, proteins, and lipids in HSV-1 virions. All UV-LEDs decreased the infectivity of HSV-1 to host cells, although 260- and 280-nm UV-LEDs had stronger inhibitory effects on HSV-1 than 310- and 365-nm UV-LEDs. In addition, the UV-LEDs targeted different viral molecules according to the peak wavelength (Fig. 6). Our study might contribute to preventing the spread of HSV-1 and other enveloped viruses using UV-LEDs.

Supplementary data to this article can be found online at https://doi.org/10.1016/j.jphotobiol.2022.112410.

## Funding

## CRediT authorship contribution statement

**Thi Kim Ngan Bui:** Writing – original draft, Writing – review & editing, Data curation, Formal analysis, Investigation. **Kazuaki Mawatari:** Conceptualization, Methodology, Validation, Formal analysis, Investigation, Writing – original draft, Writing – review & editing, Visualization, Supervision. **Takahiro Emoto:** Resources, Data curation. **Shiho Fukushima:** Methodology. **Takaaki Shimohata:** Methodology. **Takashi Uebanso:** Methodology. **Masatake Akutagawa:** Resources, Data curation. **Yohsuke Kinouchi:** Resources, Project administration, Funding acquisition. **Akira Takahashi:** Writing – review & editing, Project administration, Funding acquisition.

## Declaration of Competing Interest

The authors declare that they have no known competing financial interests or personal relationships that could have appeared to influence the work reported in this paper.

## Acknowledgments

## References

[1] Centers for Disease Control and Prevention, Website, https://www.cdc.gov/flu/pandemic-resources/basics/past-pandemics.html.

[2] The joint United Nations Programme on HIV/AIDS, Website, https://www.unaids.org/en/resources/documents/2021/UNAIDS_FactSheet.

[3] World Health Organization, Website, https://www.who.int/emergencies/diseases/novel-coronavirus-2019/situation-reports.

[4] N.H.L. Leung, Transmissibility and transmission of respiratory viruses, Nat. Rev. Microbiol. 19 (8) (2021) 528–545, https://doi.org/10.1038/s41579-021-00535-6.

[5] K. Bibby, J. Peccia, Identification of viral pathogen diversity in sewage sludge by metagenome analysis, Environ. Sci. Technol. 47 (4) (2013) 1945–1951, https://doi.org/10.1021/es305181x.

[6] L. Casanova, E. Alfano-Sobsey, W.A. Rutala, D.J. Weber, M. Sobsey, Virus transfer from personal protective equipment to healthcare employees' skin and clothing, Emerg. Infect. Dis. 14 (8) (2008) 1291–1293, https://doi.org/10.3201/eid1408.080085.

[7] N. Boschetti, M. Stucki, P.J. Späth, C. Kempf, Virus safety of intravenous immunoglobulin: future challenges, Clin. Rev. Allergy Immunol. 29 (3) (2005) 333–344, https://doi.org/10.1385/CRIAI:29:3:333.

[8] A. Gröner, C. Broumis, R. Fang, T. Nowak, B. Popp, W. Schäfer, N.J. Roth, Effective inactivation of a wide range of viruses by pasteurization, Transfusion 58 (1) (2018) 41–51, https://doi.org/10.1111/trf.14390.

[9] D.L. Martins, J. Sencar, N. Hammerschmidt, A. Flicker, J. Kindermann, T.R. Kreil, A. Jungbauer, Truly continuous low pH viral inactivation for biopharmaceutical process integration, Biotechnol. Bioeng. 117 (5) (2020) 1406–1417, https://doi.org/10.1002/bit.27292.

[10] M. Korneyeva, J. Hotta, W. Lebing, R.S. Rosenthal, L. Franks, S.R. Jr Petteway, Enveloped virus inactivation by caprylate: a robust alternative to solvent-detergent treatment in plasma derived intermediates, Biologicals 30 (2) (2002) 153–162, https://doi.org/10.1006/biol.2002.0334.

[11] E. Araud, M. Fuzawa, J.L. Shisler, J. Li, T.H. Nguyen, UV inactivation of rotavirus and tulane virus targets different components of the virions, Appl. Environ. Microbiol. 86 (4) (2020), https://doi.org/10.1128/AEM.02436-19 e02436–19.

[12] Z. Qiao, Y. Ye, P.H. Chang, D. Thirunarayanan, K.R. Wigginton, Nucleic acid photolysis by UV254 and the impact of virus encapsidation, Environ. Sci. Technol. 52 (18) (2018) 10408–10415, https://doi.org/10.1021/acs.est.8b02308.

[13] Y. Muramoto, M. Kimura, S. Nouda, Development and future of ultraviolet light-emitting diodes: UV-LED will replace the UV lamp, Semicond. Sci. Technol. 29 (8) (2014), https://doi.org/10.1088/0268-1242/29/8/084004, 084004.

[14] R. Nishisaka-Nonaka, K. Mawatari, T. Yamamoto, M. Kojima, T. Shimohata, T. Uebanso, M. Nakahashi, T. Emoto, M. Akutagawa, Y. Kinouchi, T. Wada, M. Okamoto, H. Ito, K.I. Yoshida, T. Daidoji, T. Nakaya, A. Takahashi, Irradiation by ultraviolet-light-emitting diodes inactivates influenza A viruses by inhibiting replication and transcription of viral RNA in host cells, J. Photochem. Photobiol. B 189 (2018) 193–200, https://doi.org/10.1016/j.jphotobiol.2018.10.017.

[15] M. Kojima, K. Mawatari, T. Emoto, R. Nishisaka-Nonaka, T.K.N. Bui, T. Shimohata, T. Uebanso, M. Akutagawa, Y. Kinouchi, T. Wada, M. Okamoto, H. Ito, K. Tojo, T. Daidoji, T. Nakaya, A. Takahashi, Irradiation by a combination of different peak-wavelength ultraviolet-light emitting diodes enhances the inactivation of influenza A viruses, Microorganisms 8 (7) (2020) 1014, https://doi.org/10.3390/microorganisms8071014.

[16] S.E. Beck, H. Ryu, L.A. Boczek, J.L. Cashdollar, K.M. Jeanis, J.S. Rosenblum, O.R. Lawal, K.G. Linden, Evaluating UV-C LED disinfection performance and investigating potential dual-wavelength synergy, Water Res. 109 (2017) 207–216, https://doi.org/10.1016/j.watres.2016.11.024.

[17] T. Tanaka, O. Nogariya, N. Shionoiri, Y. Maeda, A. Arakaki, Integrated molecular analysis of the inactivation of a non-enveloped virus, feline calicivirus, by UV-C radiation, J. Biosci. Bioeng. 126 (1) (2018) 63–68, https://doi.org/10.1016/j.jbiosc.2018.01.018.

[18] S.E. Beck, N.M. Hull, C. Poepping, K.G. Linden, Wavelength-dependent damage to adenoviral proteins across the germicidal UV spectrum, Environ. Sci. Technol. 52 (1) (2018) 223–229, https://doi.org/10.1021/acs.est.7b04602.

[19] T. Minamikawa, T. Koma, A. Suzuki, T. Mizuno, K. Nagamatsu, H. Arimochi, K. Tsuchiya, K. Matsuoka, T. Yasui, K. Yasutomo, M. Nomaguchi, Quantitative evaluation of SARS-CoV-2 inactivation using a deep ultraviolet light-emitting diode, Sci. Rep. 11 (1) (2021) 5070, https://doi.org/10.1038/s41598-021-84592-0.

[20] K. Oguma, S. Rattanakul, M. Masaike, Inactivation of health-related microorganisms in water using UV light-emitting diodes, Water Supply 19 (5) (2019) 1507–1514, https://doi.org/10.2166/ws.2019.022.

[21] World Health Organization, Website, https://www.who.int/news-room/fact-sheets/detail/herpes-simplex-virus.

[22] A.V. Farooq, D. Shukla, Herpes simplex epithelial and stromal keratitis: an epidemiologic update, Surv. Ophthalmol. 57 (5) (2012) 448–462, https://doi.org/10.1016/j.survophthal.2012.01.005.

[23] B.P. George, E.B. Schneider, A. Venkatesan, Encephalitis hospitalization rates and inpatient mortality in the United States, 2000–2020, PLoS One 9 (9) (2014), e104169, https://doi.org/10.1371/journal.pone.0104169.

[24] T. Takagi, J. Nishikawa, S. Fukuda, N. Kubota, Y. Kobayashi, K.I. Otsuyama, J. Nojima, H. Tsuneoka, K. Sakai, Y. Suehiro, T. Yamasaki, K. Sakurai, K. Itatani, I. Sakaida, Microbicidal effect of deep ultraviolet-light-emitting diode irradiation, Lasers Med. Sci. 36 (4) (2021) 927–931, https://doi.org/10.1007/s10103-020-03143-7.

[25] M. Nakahashi, K. Mawatari, A. Hirata, M. Maetani, T. Shimohata, T. Uebanso, Y. Hamada, M. Akutagawa, Y. Kinouchi, A. Takahashi, Simultaneous irradiation with different wavelengths of ultraviolet-light has synergistic bactericidal effect on *Vibrio parahaemolyticus*, Photochem. Photobiol. 90 (6) (2014) 1397–1403, https://doi.org/10.1111/php.12309.

[26] S.A. Connolly, J.O. Jackson, T.S. Jardetzky, R. Longnecker, Fusing structure and function: a structural view of the herpesvirus entry machinery, Nat. Rev. Microbiol. 9 (5) (2011) 369–381, https://doi.org/10.1038/nrmicro2548.

[27] P.T. Ivanova, D.S. Myers, S.B. Milne, J.L. McClaren, P.G. Thomas, H.A. Brown, Lipid composition of viral envelope of three strains of influenza virus – not all viruses are created equal, ACS Infect. Dis. 1 (9) (2015) 399–452, https://doi.org/10.1021/acsinfecdis.5b00040.

[28] R.C. Aloia, H. Tian, F.C. Jensen, Lipid composition and fluidity of the human immunodeficiency virus envelope and host cell plasma membranes, Proc. Natl. Acad. Sci. U. S. A. 90 (11) (1993) 5181–5185, https://doi.org/10.1073/pnas.90.11.5181.

[29] K. Mawatari, E. Yoshioka, S. Toda, S. Yasui, H. Furukawa, T. Shimohata, T. Ohnishi, M. Morishima, N. Harada, A. Takahashi, H. Sakaue, Y. Nakaya, Enhancement of endothelial function inhibits left atrial thrombi development in an animal model of spontaneous left atrial thrombosis, Circ. J. 78 (8) (2014) 1980–1988, https://doi.org/10.1253/circj.cj-13-1398.

[30] J. Folch, M. Lees, G.H.S. Stanley, A simple method for the isolation and purification of total lipides from animal tissues, J. Biol. Chem. 226 (1) (1957) 497–509, https://doi.org/10.1016/S0021-9258(18)64849-5.

[31] J.K. Kim, D. Patel, B.S. Choi, Contrasting structural impacts induced by cis-syn cyclobutane dimer and (6–4) adduct in dna duplex decamers: implication in mutagenesis and repair activity, Photochem. Photobiol. 62 (1) (1995) 44–50, https://doi.org/10.1111/j.1751-1097.1995.tb05236.x.

[32] T. Matsunaga, K. Hieda, O. Nikaido, Wavelength dependent formation of thymine dimers and (6–4) photoproducts in DNA by monochromatic ultraviolet-light ranging from 150 to 365 nm, Photochem. 54 (3) (1991) 403–410, https://doi.org/10.1111/j.1751-1097.1991.tb02034.x.

[33] H. Yamada, K. Hieda, Wavelength dependence (150–290 nm) of the formation of the cyclobutane dimer and the (6–4) photoproduct of thymine, Photochem. Photobiol. 55 (4) (1992) 541–548, https://doi.org/10.1111/j.1751-1097.1992.tb04276.x.

[34] É. Nascimento, S.H. da Silva, Edos R. Marques, D.W. Roberts, G.U. Braga, Quantification of cyclobutane pyrimidine dimers induced by UVB radiation in conidia of the fungi Aspergillus fumigatus, Aspergillus nidulans, Metarhizium acridum and Metarhizium robertsii, Photochem. Photobiol. 86 (6) (2010) 1259–1266, https://doi.org/10.1111/j.1751-1097.2010.00793.x.

[35] N. Bastien, J.P. Therrien, R. Drouin, Cytosine containing dipyrimidine sites can be hotspots of cyclobutane pyrimidine dimer formation after UVB exposure, Photochem. Photobiol. Sci. 12 (8) (2013) 1544–1554, https://doi.org/10.1039/c3pp50099c.

[36] T. Douki, Relative contributions of UVB and UVA to the photoconversion of (6–4) photoproducts into their dewar valence isomers, Photochem. Photobiol. 92 (4) (2016) 587–594, https://doi.org/10.1111/php.12605.

[37] A. Banyasz, T. Douki, R. Improta, T. Gustavsson, D. Onidas, I. Vayá, M. Perron, D. Markovitsi, Electronic excited states responsible for dimer formation upon UV absorption directly by thymine strands: joint experimental and theoretical study, J. Am. Chem. Soc. 134 (36) (2012) 14834–14845, https://doi.org/10.1021/ja304069f.

[38] R.M. Tyrrell, Induction of pyrimidine dimers in bacterial DNA by 365 nm radiation, Photochem. Photobiol. 17 (1) (1973) 69–73, https://doi.org/10.1111/j.1751-1097.1973.tb06334.x.

[39] S. Mouret, C. Philippe, J. Gracia-Chantegrel, A. Banyasz, S. Karpati, D. Markovitsi, T. Douki, UVA-induced cyclobutane pyrimidine dimers in DNA: a direct photochemical mechanism? Org. Biomol. Chem. 8 (7) (2010) 1706–1711, https://doi.org/10.1039/b924712b.

[40] F. Bosshard, K. Riedel, T. Schneider, C. Geiser, M. Bucheli, T. Egli, Protein oxidation and aggregation in UVA-irradiated Escherichia coli cells as signs of accelerated cellular senescence, Environ. Microbiol. 12 (11) (2010) 2931–2945, https://doi.org/10.1111/j.1462-2920.2010.02268.x.

[41] N. Zhang, J. Yan, G. Lu, Z. Guo, Z. Fan, J. Wang, Y. Shi, J. Qi, G.F. Gao, Binding of herpes simplex virus glycoprotein D to nectin-1 exploits host cell adhesion, Nat. Commun. 2 (2011) 577, https://doi.org/10.1038/ncomms1571.

[42] W.Z. Cai, P.A. Schaffer, Herpes simplex virus type 1 ICP0 plays a critical role in the de novo synthesis of infectious virus following transfection of viral DNA, J. Virol. 63 (11) (1989) 4579–4589, https://doi.org/10.1128/JVI.63.11.4579-4589.1989.

[43] W.P. Halford, C. Weisend, J. Grace, M. Soboleski, D.J. Carr, J.W. Balliet, Y. Imai, T.P. Margolis, B.M. Gebhardt, ICP0 antagonizes Stat 1-dependent repression of herpes simplex virus: implications for the regulation of viral latency, Virol. J. 3 (2006) 44, https://doi.org/10.1186/1743-422X-3-44.

[44] A. Barth, The infrared absorption of amino acid side chains, Prog. Biophys. Mol. Biol. 74 (3–5) (2000) 141–173, https://doi.org/10.1016/s0079-6107(00)00021-3.

[45] S. Prasad, I. Mandal, S. Singh, A. Paul, B. Mandal, R. Venkatramani, R. Swaminathan, Near UV-Visible electronic absorption originating from charged amino acids in a monomeric protein, Chem. Sci. 8 (8) (2017) 5416–5433, https://doi.org/10.1039/c7sc00880e.

[46] P. Wongkongkathep, H. Li, X. Zhang, R.R. Loo, R.R. Julian, J.A. Loo, Enhancing protein disulfide bond cleavage by UV excitation and electron capture dissociation for top-down mass spectrometry, Int. J. Mass Spectrom. 390 (2015) 137–145, https://doi.org/10.1016/j.ijms.2015.07.008.

[47] F. Ferrè, P. Clote, DiANNA 1.1: an extension of the DiANNA web server for ternary cysteine classification, Nucleic Acids Res. *34* (2006) W182–W185, https://doi.org/10.1093/nar/gkl189 (Web Server issue).

[48] J. McHowat, J.H. Jones, M.H. Creer, Quantitation of individual phospholipid molecular species by UV absorption measurements, J. Lipid Res. 37 (11) (1996) 2450–2460, https://doi.org/10.1016/S0022-2275(20)37493-9.

[49] T.K. Mandal, S.N. Chatterjee, Ultraviolet- and sunlight-induced lipid peroxidation in liposomal membrane, Radiat. Res. 83 (2) (1980) 290–302, https://doi.org/10.1016/S0022-2275(20)37493-9.

[50] S.N. Chatterjee, S. Agarwal, Lipid peroxidation by ultraviolet-light and high energy a particles from a cyclotron, Radiat. Environ. Biophys. 21 (4) (1983) 275–280, https://doi.org/10.1007/BF01341464.

[51] S. Grether-Beck, G. Bonizzi, H. Schmitt-Brenden, I. Felsner, A. Timmer, H. Sies, J.P. Johnson, J. Piette, J. Krutmann, Non-enzymatic triggering of the ceramide signalling cascade by solar UVA radiation, EMBO J. 19 (21) (2000) 5793–5800, https://doi.org/10.1093/emboj/19.21.5793.

[52] S. Moller-Tank, W. Maury, Phosphatidylserine receptors: enhancers of enveloped virus entryand infection, Virology 468–470 (2014) 565–580, https://doi.org/10.1016/j.virol.2014.09.009.

[53] R.T. Huang, B. Lichtenberg, O. Rick, Involvement of annexin V in the entry of influenza viruses and role of phospholipids in infection, FEBS Lett. 392 (1) (1996) 59–62, https://doi.org/10.1016/0014-5793(96)00783-1.

[54] L. Meertens, X. Carnec, M.P. Lecoin, R. Ramdasi, F. Guivel-Benhassine, E. Lew, G. Lemke, O. Schwartz, A. Amara, The TIM and TAM families of phosphatidylserine receptors mediate dengue virus entry, Cell Host Microbe 12 (4) (2012) 544–557, https://doi.org/10.1016/j.chom.2012.08.009.

[55] J. Arii, A. Fukui, Y. Shimanaka, N. Kono, H. Arai, Y. Maruzuru, N. Koyanagi, A. Kato, Y. Mori, Y. Kawaguchi, Role of phosphatidylethanolamine biosynthesis in herpes simplex virus 1-infected cells in progeny virus morphogenesis in the cytoplasm and in viral pathogenicity in vivo, J. Virol. 94 (24) (2020), https://doi.org/10.1128/JVI.01572-20 e01572–20.

[56] A. Audi, N. Soudani, G. Dbaibo, H. Zaraket, Depletion of host and viral sphingomyelin impairs influenza virus infection, Front. Microbiol. 11 (2020) 612, https://doi.org/10.3389/fmicb.2020.00612.

[57] Y. Xiao, X.N. Chu, M. He, X.C. Liu, J.Y. Hu, Impact of UVA pre-radiation on UVC DISINFECTION performance: inactivation, repair and mechanism study, Water Res. 141 (2018) 279–288, https://doi.org/10.1016/j.watres.2018.05.021.

[58] K. Song, F. Taghipour, M. Mohseni, Microorganisms inactivation by wavelength combinations of ultraviolet-light-emitting diodes (UV-LEDs), Sci. Total Environ. 665 (2019) 1103–1110, https://doi.org/10.1016/j.scitotenv.2019.02.041.

[59] G.Q. Li, W.L. Wang, Z.Y. Huo, Y. Lu, H.Y. Hu, Comparison of UV-LED and low pressure UV for water disinfection: photoreactivation and dark repair of *Escherichia coli*, Water Res. 126 (2017) 134–143, https://doi.org/10.1016/j.watres.2017.09.030.